JHEP

Published for SISSA by Springer

Received: April 15, 2010
Accepted: May 3, 2010
Published: May 20, 2010

HQET at order $1/m$: II. Spectroscopy in the quenched approximation

ALPHA Collaboration

Benoît Blossier,[a] **Michele Della Morte,**[b] **Nicolas Garron,**[c,d] **Georg von Hippel,**[b,e] **Tereza Mendes,**[e,f] **Hubert Simma**[e] **and Rainer Sommer**[e]

[a] *Laboratoire de Physique Théorique, Bâtiment 210, Université Paris XI, F-91405 Orsay Cedex, France*

[b] *Institut für Kernphysik, University of Mainz, D-55099 Mainz, Germany*

[c] *Departamento de Física Teórica and Instituto de Física Teórica IFT-UAM/CSIC, Universidad Autónoma de Madrid, Cantoblanco 28049 Madrid, Spain*

[d] *SUPA, School of Physics, University of Edinburgh, Edinburgh EH9 3JZ, U.K.*

[e] *NIC, DESY, Platanenallee 6, 15738 Zeuthen, Germany*

[f] *IFSC, University of São Paulo, C.P. 369, CEP 13560-970, São Carlos SP, Brazil*

E-mail: benoit.blossier@th.u-psud.fr, morte@kph.uni-mainz.de, ngarron@staffmail.ed.ac.uk, hippel@kph.uni-mainz.de, mendes@ifsc.usp.br, hubert.simma@desy.de, rainer.sommer@desy.de

Abstract: Using Heavy Quark Effective Theory with non-perturbatively determined parameters in a quenched lattice calculation, we evaluate the splittings between the ground state and the first two radially excited states of the B_s system at static order. We also determine the splitting between first excited and ground state, and between the B_s^* and B_s ground states to order $1/m_b$. The Generalized Eigenvalue Problem and the use of all-to-all propagators are important ingredients of our approach.

Keywords: Lattice QCD, B-Physics, Heavy Quark Physics

doi:10.1007/JHEP05(2010)074

JHEP05(2010)074

Contents

1 Introduction 1

2 Methodological background 2
- 2.1 Non-perturbative HQET 2
- 2.2 The generalized eigenvalue problem 3
- 2.3 Mass splittings to $O(1/m_b)$ 4

3 Simulation details and results 4
- 3.1 Lattice parameters 4
- 3.2 Measurements of correlation functions 5
- 3.3 Determination of energies 5
- 3.4 Continuum limit 7
- 3.5 Results 10

4 Conclusions 11

A All-to-all propagators 12
- A.1 Even-odd preconditioning 12
- A.2 Approximate low modes and a stochastic estimator 13
- A.3 Time dilution 14

1 Introduction

In recent years, there has been significant progress in determining the spectrum of hadrons containing a b quark, both experimentally [1–5], and on the lattice [6–10]. A comparison of theory and experiment is of considerable interest for these hydrogen-like systems, in particular since Heavy Quark Effective Theory (HQET) [11–14] is applicable and is at the same time an important theoretical tool to isolate new physics in the flavor sector [15].

The extraction of information on excited states from lattice simulations is a difficult problem, since the excited states appear as subleading exponentially decaying contributions to the lattice correlators, which at large times are dominated by the ground state and at small times by the combined contributions of arbitrarily highly excited states, and on top of this are affected by noise. A number of different methods [16–19] have been proposed for overcoming this challenge; recently we have shown that with an efficient use of the generalized eigenvalue problem (GEVP), rigorous statements about the systematic error caused by the admixture of other states can be proven [20]. In particular, we have shown that for a suitable choice of Euclidean times t and t_0, the systematic error decays exponentially with an exponent given by an energy gap that can be made large by an appropriately chosen variational basis.

JHEP05(2010)074

Since their Compton wavelength is much shorter than any realistically achievable lattice spacing, b quarks cannot be simulated as relativistic quarks on a lattice. A description of heavy-light mesons that is suitable for use in the context of lattice QCD simulations is given by HQET with non-perturbatively determined parameters [21, 22]. The parameters necessary to match HQET to QCD at order $\mathrm{O}(1/m_\mathrm{b})$ have been determined in the quenched approximation by our collaboration [23], and the non-perturbative determination for QCD with $N_\mathrm{f} = 2$ dynamical quark flavors is far advanced [24].

In this paper, we present our results for the heavy-light meson spectrum from HQET using the GEVP method. In section 2, we give a brief review of our methods. Details of the simulations and data analysis procedures are given in section 3, and our results for the quenched heavy-light spectrum are presented. Section 4 contains our conclusions. Some technical details of our implementation of all-to-all propagators are relegated to the appendix.

2 Methodological background

2.1 Non-perturbative HQET

HQET on the lattice offers a theoretically rigorous approach to the physics of B-mesons since it is based on a strict expansion of QCD correlation functions in powers of $1/m_\mathrm{b}$ around the limit $m_\mathrm{b} \to \infty$. Subleading effects are described by insertions of higher dimensional operators whose coupling constants are formally $\mathrm{O}(1/m_\mathrm{b})$ to the appropriate power. This means that HQET can be renormalized and matched to QCD in a completely non-perturbative way [25], implying the existence of the continuum limit at any fixed order in the $1/m_\mathrm{b}$ expansion.

To fix the notation we write the HQET action at $\mathrm{O}(1/m_\mathrm{b})$ as

$$S_\mathrm{HQET} = a^4 \sum_x \{\mathcal{L}_\mathrm{stat}(x) - \omega_\mathrm{kin}\mathcal{O}_\mathrm{kin}(x) - \omega_\mathrm{spin}\mathcal{O}_\mathrm{spin}(x)\} \,, \tag{2.1}$$

$$\mathcal{L}_\mathrm{stat}(x) = \overline{\psi}_\mathrm{h}(x)\,(D_0 + \delta m)\,\psi_\mathrm{h}(x)\,, \tag{2.2}$$

$$\mathcal{O}_\mathrm{kin}(x) = \overline{\psi}_\mathrm{h}(x)\mathbf{D}^2\psi_\mathrm{h}(x)\,, \quad \mathcal{O}_\mathrm{spin}(x) = \overline{\psi}_\mathrm{h}(x)\sigma\cdot\mathbf{B}\psi_\mathrm{h}(x)\,, \tag{2.3}$$

where ψ_h satisfies $\frac{1+\gamma_0}{2}\psi_\mathrm{h} = \psi_\mathrm{h}$. The parameters ω_kin and ω_spin are of order $1/m_\mathrm{b}$, and δm is the counter-term absorbing the power-divergences of the static quark self energy. The signal-to-noise ratio of large-distance correlation functions is significantly improved by replacing the link $U(x,0)$ in the backward covariant derivative $D_0 f(x) = [f(x) - U^\dagger(x - a\hat{0}, 0)\; f(x - a\hat{0})]/a$, with a smeared link [26].

Exponentiating the action of eq. (2.1) would give (non-renormalizable) NRQCD [27]; in order to retain the renormalizability of the static theory, we treat the theory in a strict expansion in $1/m_\mathrm{b}$, where the $\mathrm{O}(1/m_\mathrm{b})$ parts of the action appear as insertions in correlation functions. For the expectation value of some operator O this means (ignoring the possibility of explicit $1/m_\mathrm{b}$ operator corrections, which do not affect the energy levels [23])

$$\langle O\rangle = \langle O\rangle_\mathrm{stat} + \omega_\mathrm{kin}\, a^4 \sum_x \langle O\, \mathcal{O}_\mathrm{kin}(x)\rangle_\mathrm{stat} + \omega_\mathrm{spin}\, a^4 \sum_x \langle O\, \mathcal{O}_\mathrm{spin}(x)\rangle_\mathrm{stat} \tag{2.4}$$

JHEP05(2010)074

where $\langle O \rangle_{\rm stat}$ denotes the expectation value in the static approximation.

To fully specify HQET, the parameters δm, $\omega_{\rm kin}$ and $\omega_{\rm spin}$ must be determined by matching to QCD. In order to retain the asymptotic convergence in $1/m_{\rm b}$, this matching must be done non-perturbatively, since for a perturbative matching at loop order l, the $\mathrm{O}(g^{2l})$ truncation error of the static term is much larger than the power corrections to the static limit:

$$\epsilon_{\rm pert}(l) \propto \bar{g}^{2l}\,(m_{\rm b}) \propto [2b_0 \log(m_{\rm b}/\Lambda_{\rm QCD})]^{-l} \underset{m_{\rm b}\to\infty}{\gg} \frac{\Lambda_{\rm QCD}}{m_{\rm b}}\,. \tag{2.5}$$

A fully non-perturbative determination of the parameters of HQET has been carried out in [23]. Here we employ the same discretization of QCD and HQET and in particular the determined values of $\omega_{\rm kin}$ and $\omega_{\rm spin}$. For further details of the matching and discretization, the reader is referred to [23].

2.2 The generalized eigenvalue problem

In this section, we recall the relevant contents of [20]. Starting from some fields $O_i(x)$ localised on a time slice and their momentum zero projection $a^3 \sum_{\mathbf{x}} O_i(x) = \tilde{O}_i(x_0)$, a matrix of Euclidean space correlation functions,

$$\begin{aligned} C_{ij}(t) &= \langle \tilde{O}_i(t) \tilde{O}_j^*(0) \rangle = \sum_{n=1}^{\infty} \mathrm{e}^{-E_n t} \psi_{ni} \psi_{nj}^*\,, \quad i,j = 1,\ldots,N \\ \psi_{ni} &\equiv (\psi_n)_i = \langle 0|\hat{O}_i|n\rangle \quad E_n < E_{n+1}\,, \end{aligned} \tag{2.6}$$

provides the basis for the GEVP

$$C(t)\, v_n(t,t_0) = \lambda_n(t,t_0)\, C(t_0)\, v_n(t,t_0)\,, \quad n = 1,\ldots,N\,, \quad t > t_0\,. \tag{2.7}$$

Effective energies for the n-th energy level are given by

$$E_n^{\rm eff}(t,t_0) = -\partial_t \log \lambda_n(t,t_0) \equiv -\frac{1}{a}\left[\log \lambda_n(t+a,t_0) - \log \lambda_n(t,t_0)\right], \tag{2.8}$$

where a is the lattice spacing. Provided that $t_0 > t/2$, the effective energies converge to the exact energy levels as [20]

$$E_n^{\rm eff}(t,t_0) = E_n + \mathrm{O}(\mathrm{e}^{-\Delta E_{N+1,n}\, t})\,, \quad \Delta E_{m,n} = E_m - E_n. \tag{2.9}$$

In HQET, all correlation functions

$$C_{ij}(t) = C_{ij}^{\rm stat}(t) + \omega_{\rm kin}\, C_{ij}^{\rm kin}(t) + \omega_{\rm spin}\, C_{ij}^{\rm spin}(t) + \mathrm{O}(\omega^2) \tag{2.10}$$

are computed in an expansion in a small parameter, $\omega \propto 1/m_{\rm b}$. Correspondingly, the energy levels expand as

$$E_n^{\rm eff}(t,t_0) = E_n^{\rm eff,stat}(t,t_0) + \omega_{\rm x} E_n^{\rm eff,x}(t,t_0) + \mathrm{O}(\omega^2) \tag{2.11}$$

$$E_n^{\rm eff,stat}(t,t_0) = a^{-1} \log \frac{\lambda_n^{\rm stat}(t,t_0)}{\lambda_n^{\rm stat}(t+a,t_0)} \tag{2.12}$$

$$E_n^{\rm eff,x}(t,t_0) = \frac{\lambda_n^{\rm x}(t,t_0)}{\lambda_n^{\rm stat}(t,t_0)} - \frac{\lambda_n^{\rm x}(t+a,t_0)}{\lambda_n^{\rm stat}(t+a,t_0)} \tag{2.13}$$

JHEP05(2010)074

where $\mathrm{x} \in \{\mathrm{kin}, \mathrm{spin}\}$, with the behavior at large time $t \leq 2t_0$,

$$E_n^{\mathrm{eff,stat}}(t,t_0) = E_n^{\mathrm{stat}} + \beta_n^{\mathrm{stat}}\, \mathrm{e}^{-\Delta E^{\mathrm{stat}}_{N+1,n}\, t} + \dots\,, \tag{2.14}$$

$$E_n^{\mathrm{eff,x}}(t,t_0) = E_n^{\mathrm{x}} + [\,\beta_n^{\mathrm{x}} - \beta_n^{\mathrm{stat}}\, t\, \Delta E^{\mathrm{x}}_{N+1,n}\,]\mathrm{e}^{-\Delta E^{\mathrm{stat}}_{N+1,n}\, t} + \dots\,. \tag{2.15}$$

where

$$C^{\mathrm{stat}}(t)\, v_n^{\mathrm{stat}}(t,t_0) = \lambda_n^{\mathrm{stat}}(t,t_0)\, C^{\mathrm{stat}}(t_0)\, v_n^{\mathrm{stat}}(t,t_0)\,, \tag{2.16}$$

$$\frac{\lambda_n^{\mathrm{x}}(t,t_0)}{\lambda_n^{\mathrm{stat}}(t,t_0)} = \big(v_n^{\mathrm{stat}}(t,t_0)\,,\, [[\lambda_n^{\mathrm{stat}}(t,t_0)]^{-1}\, C^{\mathrm{x}}(t) - C^{\mathrm{x}}(t_0)] v_n^{\mathrm{stat}}(t,t_0)\big)\,.$$

with $(v_m^{\mathrm{stat}}(t,t_0)\,,\, C^{\mathrm{stat}}(t_0)\, v_n^{\mathrm{stat}}(t,t_0)) = \delta_{mn}$. We note that the GEVP is only ever solved for the static correlator matrices.

2.3 Mass splittings to $\mathrm{O}(1/m_{\mathrm{b}})$

With the static Lagrangian eq. (2.2), all HQET energies satisfy exactly $E_n = E_n|_{\delta m=0} + \frac{1}{a}\log(1+a\delta m)$, and the power divergent δm drops out in energy differences. Since we only consider these in this paper, we need just ω_{kin} and ω_{spin} of [23].

The excitation energies at the static order of HQET are given simply by the differences of the static energies,

$$\Delta E_{n,1}^{\mathrm{stat}} = E_n^{\mathrm{stat}} - E_1^{\mathrm{stat}}\,, \tag{2.17}$$

and at order $1/m_{\mathrm{b}}$, the excitation energies of pseudoscalar $\mathrm{B_s}$ states become

$$\Delta E_{n,1}^{\mathrm{HQET}} = (E_n^{\mathrm{stat}} - E_1^{\mathrm{stat}}) + \omega_{\mathrm{kin}}(E_n^{\mathrm{kin}} - E_1^{\mathrm{kin}}) + \omega_{\mathrm{spin}}(E_n^{\mathrm{spin}} - E_1^{\mathrm{spin}})\,. \tag{2.18}$$

At the static order, the masses of pseudoscalar and vector states are degenerate due to spin symmetry [13]. This degeneracy is lifted at the $\mathrm{O}(1/m_{\mathrm{b}})$ level by the contribution from $\mathcal{O}_{\mathrm{spin}}$, giving a $\mathrm{B_s} - \mathrm{B_s^*}$ mass difference of

$$\Delta E_{\mathrm{P-V}} = \frac{4}{3}\omega_{\mathrm{spin}} E_1^{\mathrm{spin}}\,. \tag{2.19}$$

3 Simulation details and results

3.1 Lattice parameters

We use three quenched ensembles of 100 configurations each, generated using the Wilson gauge action with parameters $\beta = 6.0219$, 6.2885 and 6.4956. The physical volume was kept constant at $L \approx 1.5\,\mathrm{fm}$, leading to $L/a = 16$, 24, 32 for the three ensembles. We used time extent $T = 2L$ throughout.

The static quark is discretized on each ensemble with both the HYP1 and HYP2 [26, 28, 29] actions. The light valence quark is discretized by a non-perturbatively $\mathrm{O}(a)$-improved Wilson action [30, 31], and its mass was fixed to the strange quark mass, giving $\kappa_s = 0.133849$, 0.1349798, 0.1350299, respectively [32]. A summary of the simulation parameters used, with the corresponding values of ω_{kin} and ω_{spin}, is given in table 1.

JHEP05(2010)074

β	r_0/a	$(L/a)^3 \times T/a$	κ_s	N_L	N_η	ω_kin/a	ω_spin/a
6.0219	5.57	$16^3 \times 32$	0.133849	50	2	0.321(7)	0.54(3)
6.2885	8.38	$24^3 \times 48$	0.1349798	50	2	0.425(10)	0.70(4)
6.4956	11.03	$32^3 \times 64$	0.1350299	0	4	0.534(13)	0.86(4)

Table 1. Parameters of the simulations: inverse coupling β, approximate value of the scale parameter r_0 [33] in lattice units, spacetime volume, hopping parameter for the strange quark mass [32], number of low-lying eigenmodes and number of noise sources used in the all-to-all [34] estimate of the strange quark propagators, and approximate values of the HQET couplings ω_kin and ω_spin in lattice units.

3.2 Measurements of correlation functions

The strange quark propagators are computed through a variant of the Dublin all-to-all method [34]. We use approximate instead of exact low modes (the method remains exact) and employ even-odd preconditioning in order to reduce the size of the stochastically estimated inverse of the Dirac operator by a factor of 2. The reader is referred to appendix A for details.

The interpolating fields are constructed using quark bilinears

$$\begin{aligned} O_k(x) &= \overline{\psi}_\mathrm{h}(x)\gamma_0\gamma_5\psi_\mathrm{l}^{(k)}(x) \\ O_k^*(x) &= \overline{\psi}_\mathrm{l}^{(k)}(x)\gamma_0\gamma_5\psi_\mathrm{h}(x) \end{aligned} \tag{3.1}$$

built from the static quark field $\psi_\mathrm{h}(x)$ and different levels of Gaussian smearing [35] for the light quark field

$$\psi_\mathrm{l}^{(k)}(x) = \left(1 + \kappa_\mathrm{G}\, a^2\, \Delta\right)^{R_k} \psi_\mathrm{l}(x)\,, \tag{3.2}$$

where the gauge fields in the covariant Laplacian Δ are first smeared with 3 iterations of (spatial) APE smearing [36, 37] to reduce noise. At $\beta = 6.2885$, we use $R_k = 0$, 22, 45, 67, 90, 135, 180, 225 with $\kappa_\mathrm{G} = 0.1$. At the other values of β, we rescale the values of R_k used so that the physical size $r_{\mathrm{phys},k} \approx 2a\sqrt{\kappa_\mathrm{G} R_k}$ of the wavefunctions is kept fixed; in particular we keep $r_\mathrm{max} = r_{\mathrm{phys},7} \approx 0.6\,\mathrm{fm}$.

For these bilinears, we compute the following correlators:

$$\begin{aligned} C_{ij}^\mathrm{stat}(t) &= \sum_{x,\mathbf{y}} \left\langle O_i(x_0+t,\mathbf{y})\, O_j^*(x)\right\rangle_\mathrm{stat}\,, \\ C_{ij}^\mathrm{kin/spin}(t) &= \sum_{x,\mathbf{y},z} \left\langle O_i(x_0+t,\mathbf{y})\, O_j^*(x)\, \mathcal{O}_\mathrm{kin/spin}(z)\right\rangle_\mathrm{stat} \end{aligned} \tag{3.3}$$

with the $\mathrm{O}(1/m_\mathrm{b})$ fields defined in eq. (2.3).

3.3 Determination of energies

The correlator matrices of eq. (3.3) are "thinned" to form a sequence of $N \times N$ matrices, where $N \in \{2, \ldots, 7\}$, by selecting only entries from a certain subset $\mathcal{I}_N$ of indices where

JHEP05(2010)074

n	2	3	4	5	6
$r_0(E_n^{\rm stat} - E_1^{\rm stat})$	1.50(5)	2.7(1)	4.0	5.0	6.0

Table 2. Rough estimate of the static spectrum. For $n \leq 3$, the gaps come from the continuum limit; for $n \geq 4$, the rough estimate used to stabilize the fit is quoted.

$\mathcal{I}_N = \{1,7\}$, $\{1,4,7\}$, $\{1,3,5,7\}$, $\{1,2,4,6,7\}$, $\{1,2,3,5,6,7\}$, $\{1,2,3,4,5,6,7\}$. An alternative procedure, used in [20] is "pruning" [38], where the $N \times N$ matrices are formed by projection onto the subspaces spanned by the lowest N eigenvectors of $C(t_i)$ for some small t_i. We decided not to use this version since it introduces a dependence on the relative normalization of the fields O_i. Moreover, with thinning we found a somewhat faster convergence to the plateau for the ground state energy compared to the pruning version [39] when the normalization of O_i in [20] is used. We note that the fact that we found the same low-lying energy levels with thinning as with pruning is a further confirmation that the GEVP is quite robust against changes of the variational basis employed.

For each of the resulting $N \times N$ correlator matrices, we solve the static GEVP and compute the static and $\mathrm{O}(1/m_{\rm b})$ energies. This gives a series of estimates $E_n^{\rm eff,stat}(N,t,t_0)$, $E_n^{\rm eff,kin}(N,t,t_0)$ and $E_n^{\rm eff,spin}(N,t,t_0)$ with associated statistical errors, which we determine by a full Jackknife analysis.

To arrive at final numbers for E_n we also need to estimate the size of the systematic errors coming from the higher excited states. To do this, we first perform a fit of the form

$$\begin{aligned} E_n^{\rm eff,stat}(N,t,t_0) &= E_n^{\rm stat} + \epsilon_n^{N,\rm stat}(t) \\ &= E_n^{\rm stat} + \beta_{n,N}^{\rm stat} \mathrm{e}^{-(E_{N+1}^{\rm stat} - E_n^{\rm stat})t} \end{aligned} \tag{3.4}$$

to the GEVP results for $E_n^{\rm eff,stat}(N,t,t_0)$, fitting the data at $N = 3,\ldots,5$, $\frac{1}{2}r_0 < t_0 \leq 6a$, $t_0 \leq t \leq 2t_0$ and $n = 1,\ldots,6$ simultaneously. The stability of the fit is enhanced in the following manner: First we perform an unconstrained fit to extract $E_n^{\rm stat} - E_1^{\rm stat}$ for $n = 4,5,6$ for each lattice spacing and action and compute a rough average of $r_0(E_n^{\rm stat} - E_1^{\rm stat})$ for these values of n. Then we repeat the fit, constraining $r_0(E_n^{\rm stat} - E_1^{\rm stat})$ for $n \geq 4$ to the previous average (this renders the fit linear). For $n \leq 3$ this is unnecessary as these levels are well determined at each individual lattice spacing. We list the extracted values of $r_0(E_n^{\rm stat} - E_1^{\rm stat})$ in table 2.

Finally, using the values of $E_n^{\rm stat}$ and $\beta_{n,N}^{\rm stat}$ determined from this fit as (fixed) input parameters, we fit $E_n^{\rm eff,kin}(N,t,t_0)$ and $E_n^{\rm eff,spin}(N,t,t_0)$ by

$$\begin{aligned} E_n^{\rm eff,kin}(N,t,t_0) &= E_n^{\rm kin} + \epsilon_n^{N,\rm kin}(t) \\ &= E_n^{\rm kin} + \left[\beta_{n,N}^{\rm kin} - \beta_{n,N}^{\rm stat}\, t\, (E_{N+1}^{\rm kin} - E_n^{\rm kin})\right] \mathrm{e}^{-(E_{N+1}^{\rm stat} - E_n^{\rm stat})t} \end{aligned} \tag{3.5}$$

$$\begin{aligned} E_n^{\rm eff,spin}(N,t,t_0) &= E_n^{\rm spin} + \epsilon_n^{N,\rm spin}(t) \\ &= E_n^{\rm spin} + \left[\beta_{n,N}^{\rm spin} - \beta_{n,N}^{\rm stat}\, t\, (E_{N+1}^{\rm spin} - E_n^{\rm spin})\right] \mathrm{e}^{-(E_{N+1}^{\rm stat} - E_n^{\rm stat})t} \end{aligned} \tag{3.6}$$

in the same manner.

While the fitted results are quite stable, we consider them as rough estimates only, since our fits include only the leading exponential correction, and there are systematic

JHEP05(2010)074

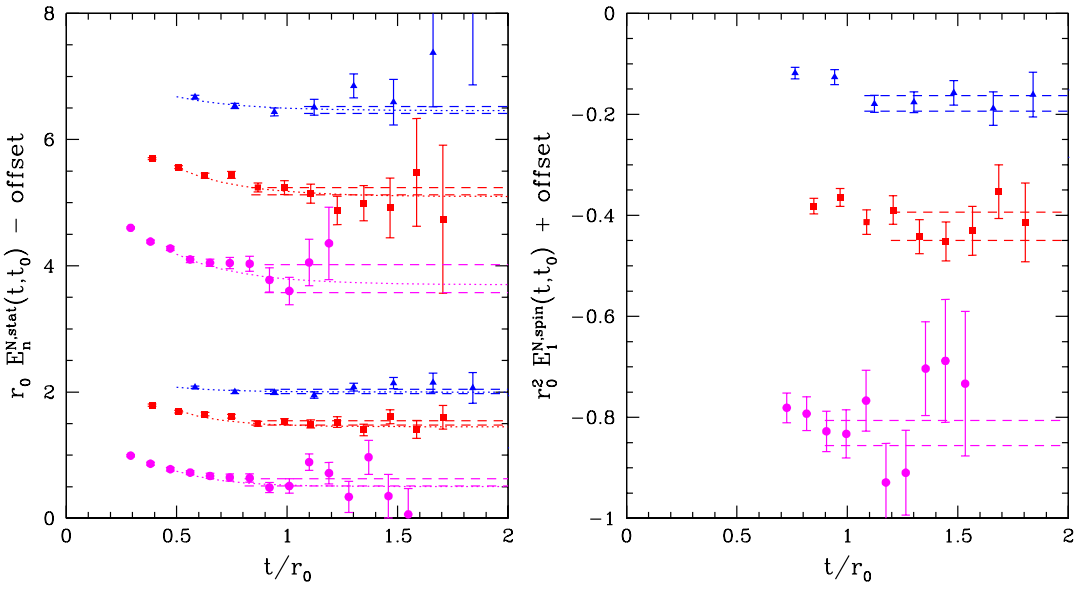

Figure 1. Illustration of some plateaux. Left: $E_2^{N\mathrm{stat}}$ (bottom half) and $E_3^{N\mathrm{stat}}$ (upper half). Here $N = 5$ and within each group the lattice spacing is decreasing from top to bottom. Dotted lines represent the global fit, while dashed lines indicate the chosen plateau. Right: the ground state spin splitting. The ordinates of the points are shifted by an arbitrary β-dependent offset in order to make the different plateaux visible separately.

effects from higher corrections to the GEVP. We therefore employ the fits only to estimate the size of the leading corrections. For a reliable estimate of the energy levels, we calculate plateau averages from $t = t_{\mathrm{min}} \geq t_0$ on at each N and t_0, and take as our final estimate that plateau average for which the sum $\sigma_{\mathrm{tot}} = \sigma_{\mathrm{stat}} + \sigma_{\mathrm{sys}}$ of the statistical error σ_{stat} of the plateau average and the maximum systematic error $\sigma_{\mathrm{sys}} = \epsilon(t_{\mathrm{min}})$ becomes minimal, subject to the constraint that $\sigma_{\mathrm{sys}} < \frac{1}{3}\sigma_{\mathrm{stat}}$. We impose the latter constraint in order to ensure that the total error is dominated by statistical errors.

An illustration of the more problematic plateaux is shown in figure 1. It is rather clear that without some analysis of corrections due to excited states it is very difficult to locate a safe plateau region at least for $n = 3$.

Our results are given in table 3; besides the plateaux found by the method described in the preceding paragraph, we also show the results of the global fit, which in almost all cases agrees very well with the final plateau value.

3.4 Continuum limit

We now turn to the continuum extrapolation of the level splittings. Using the fact that the static actions employed are discretizations of the same continuum theory, we perform a combined continuum limit by fitting a function of the form ($k = 1, 2$ for HYP1, HYP2 actions)

$$\Phi_{i,k}(a/r_0) = \Phi_i + c_{i,k}(a/r_0)^{s_i} \tag{3.7}$$

JHEP05(2010)074

		HYP1		HYP2	
β	Observable	Fit	Plateau	Fit	Plateau
6.0219	$aE_1^{\rm stat}$	0.4407(2)	0.441(1)	0.4081(2)	0.409(1)
	$aE_2^{\rm stat}$	0.708(2)	0.711(5)	0.678(2)	0.680(6)
	$aE_3^{\rm stat}$	0.893(5)	0.92(2)	0.868(5)	0.89(2)
	$a^2E_1^{\rm kin}$	0.743(1)	0.740(2)	0.774(1)	0.771(2)
	$a^2E_2^{\rm kin}$	0.843(8)	0.85(1)	0.859(7)	0.88(1)
	$a^2E_1^{\rm spin}$	-0.0300(5)	-0.0293(7)	-0.0285(4)	-0.0279(8)
	$a^2E_2^{\rm spin}$	-0.026(2)	-0.029(3)	-0.023(2)	-0.025(2)
6.2885	$aE_1^{\rm stat}$	0.3319(2)	0.3328(7)	0.3032(2)	0.3041(7)
	$aE_2^{\rm stat}$	0.507(1)	0.515(4)	0.478(1)	0.485(4)
	$aE_3^{\rm stat}$	0.648(3)	0.67(1)	0.614(3)	0.625(7)
	$a^2E_1^{\rm kin}$	0.6479(5)	0.6481(4)	0.6743(4)	0.6745(3)
	$a^2E_2^{\rm kin}$	0.682(4)	0.68(1)	0.704(4)	0.70(1)
	$a^2E_1^{\rm spin}$	-0.0127(1)	-0.0126(2)	-0.0129(1)	-0.0130(3)
	$a^2E_2^{\rm spin}$	-0.0115(9)	-0.011(1)	-0.011(1)	-0.012(1)
6.4956	$aE_1^{\rm stat}$	0.2742(3)	0.275(1)	0.2482(3)	0.249(1)
	$aE_2^{\rm stat}$	0.409(2)	0.405(8)	0.384(2)	0.381(8)
	$aE_3^{\rm stat}$	0.518(3)	0.52(2)	0.491(3)	0.50(2)
	$a^2E_1^{\rm kin}$	0.5999(5)	0.5997(3)	0.6240(3)	0.6229(7)
	$a^2E_2^{\rm kin}$	0.620(3)	0.625(6)	0.645(2)	0.645(4)
	$a^2E_1^{\rm spin}$	-0.0081(1)	-0.0079(5)	-0.0076(1)	-0.0074(4)
	$a^2E_2^{\rm spin}$	-0.0108(9)	-0.005(4)	-0.0098(8)	-0.007(2)

Table 3. The measured values of the HQET energies in lattice units. Shown are both the values obtained from a global fit ("Fit") and from our more conservative plateau selection ("Plateau") as described in the text, for both the HYP1 and HYP2 discretization of the heavy quark.

to our dimensionless quantitites $\Phi_i \in \{r_0\Delta E_{2,1}^{\rm stat}, r_0\Delta E_{3,1}^{\rm stat}, r_0\Delta E_{\rm P-V}, r_0\Delta E_{2,1}^{\rm HQET}\}$. Since O($a$)-improvement is fully implemented in the static approximation, we use powers $s_1 = s_2 = 2$. On the other hand, the $1/m_{\rm b}$ corrections have O(a) discretization errors, yielding $s_3 = 1$ for the observable $\Delta E_{\rm P-V}$. For $\Delta E_{n,1}^{\rm HQET}$, there are two possible ways of taking the continuum limit. First we extrapolate $\Delta E_{n,1}^{\rm stat}$ and the O($1/m_{\rm b}$) contribution separately to $a \to 0$ and add the continuum limits afterwards. Here we set $s_4^{\rm stat} = 2$ for the static part and $s_4^{1/m} = 1$ for the O($1/m_{\rm b}$) correction. Second, one can form the combined $\Delta E_{n,1}^{\rm HQET}$ at each β and take the continuum limit of the combination. The linear term in a which is present in the combined data, is suppressed by a factor $1/m_{\rm b}$. Given in addition the flatness of the data in a (see figure 2) we just use $s_4 = 2$ for the combination, assuming that this term dominates.

Figure 2 shows the approach to the continuum limit for the static and full HQET energy splittings. The results for HYP1 and HYP2 are distinguished by color; the static splittings are shown as circles, whereas the full HQET splitting $\Delta E_{2,1}^{\rm HQET}$ is shown as diamonds. Also shown are the fits to the continuum limit together with their error bands. We see that

JHEP05(2010)074

		$\beta = 6.0219$	$\beta = 6.2885$	$\beta = 6.4956$	cont. limit
$r_0\Delta E_{2,1}^{\mathrm{stat}}$	HYP1	1.50(3)	1.52(9)	1.46(8)	1.50(5)
	HYP2	1.51(3)	1.51(3)	1.47(8)	
$r_0\Delta E_{3,1}^{\mathrm{stat}}$	HYP1	2.67(10)	2.78(9)	2.7(2)	2.7(1)
	HYP2	2.72(10)	2.68(6)	2.8(2)	
$r_0\Delta E_{2,1}^{1/m}$	HYP1	0.20(2)	0.14(4)	0.17(5)	0.03(6)
	HYP2	0.21(2)	0.08(4)	0.13(3)	
$r_0\Delta E_{2,1}^{\mathrm{HQET}}$	HYP1	1.70(4)	1.66(6)	1.63(10)	1.56(8)
	HYP2	1.72(4)	1.59(6)	1.59(9)	
$r_0\Delta E_{2,1}^{\mathrm{stat}}\big\vert_{\mathrm{continuum}} + r_0\Delta E_{2,1}^{1/m}\big\vert_{\mathrm{continuum}}$					1.54(9)
$r_0\Delta E_{\mathrm{P-V}}$	HYP1	-0.093(7)	-0.083(6)	-0.089(8)	-0.075(8)
	HYP2	-0.114(9)	-0.103(8)	-0.092(7)	

Table 4. The energy level differences in units of the scale r_0. Shown are the results at each β for both static-quark actions, together with their common continuum limit.

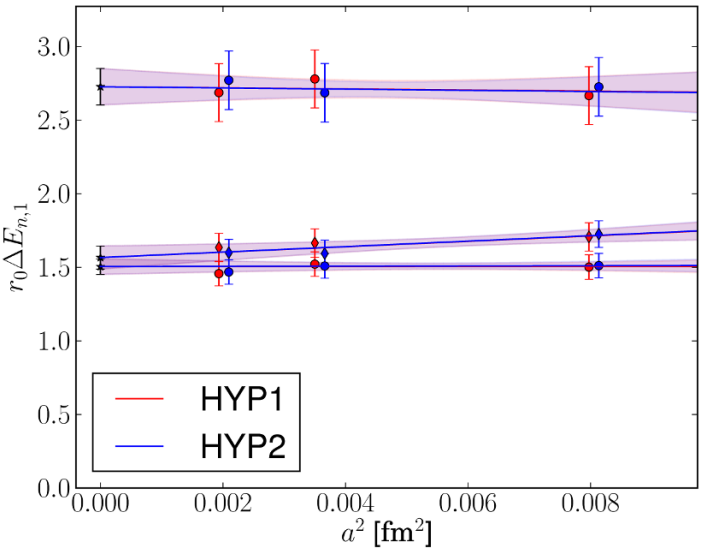

Figure 2. Plot of the continuum limits (stars) of $\Delta E_{n,1}^{\mathrm{stat}}$ (circles) and $\Delta E_{2,1}^{\mathrm{HQET}}$ (diamonds). Shown are the results for both HYP1 (red, shifted to the left) and HYP2 (blue, shifted to the right).

the approach to the continuum limit is rather flat in particular for $\Delta E_{2,1}$, and that the $\mathrm{O}(1/m_{\mathrm{b}})$ corrections constitute only a small shift of the energy splitting between the first excited and ground states. In figure 3 we show the approach to the continuum limit for the spin splitting $\Delta E_{\mathrm{P-V}}$ in the same fashion.

JHEP05(2010)074

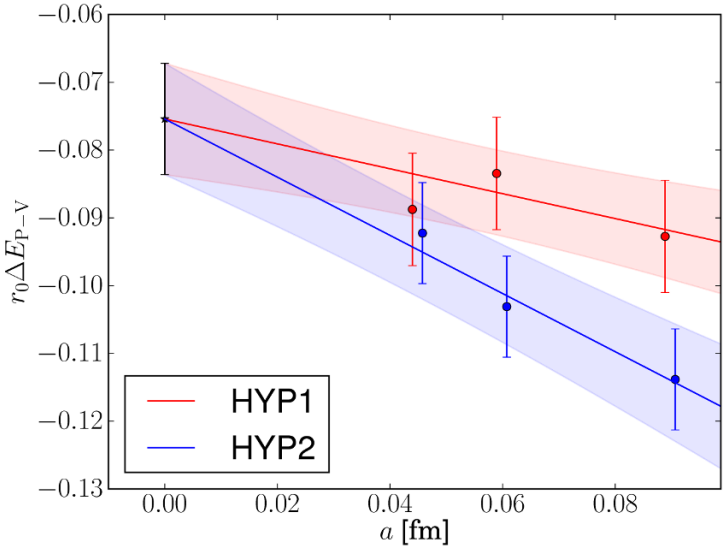

Figure 3. Plot of the continuum limit (star) of $\Delta E_{\mathrm{P-V}}$ for HYP1 (red, shifted to the left) and HYP2 (blue, shifted to the right).

3.5 Results

Our findings for the continuum values of the level splittings are summarized in table 4.

For the static spectrum, we obtain

$$r_0\Delta E^{\mathrm{stat}}_{2,1} = 1.50(5) \tag{3.8}$$

$$r_0\Delta E^{\mathrm{stat}}_{3,1} = 2.7(1)\,, \tag{3.9}$$

corresponding (using $r_0 = 0.5\,\mathrm{fm}$) to $\Delta E^{\mathrm{stat}}_{2,1} = 594(21)\,\mathrm{MeV}$ and $\Delta E^{\mathrm{stat}}_{3,1} = 1076(48)\,\mathrm{MeV}$ in good agreement with the results of [10] at a fixed lattice spacing. These numbers in physical units are meant as a rough illustration, since no quenching error is attached to them.

At $\mathrm{O}(1/m_{\mathrm{b}})$, we obtain $r_0\Delta E^{\mathrm{HQET}}_{2,1} = 1.54(9)$ when taking separate continuum limits for the static and $\mathrm{O}(1/m_{\mathrm{b}})$ energy differences, and

$$r_0\Delta E^{\mathrm{HQET}}_{2,1} = 1.56(8) \tag{3.10}$$

when combining static and $\mathrm{O}(1/m_{\mathrm{b}})$ energy levels before taking the continuum limit. The results from both procedures agree within errors, indicating that the $\mathrm{O}(a)$ term omitted in the combined extrapolation is at most a minor source of systematic error. In physical units (again using $r_0 = 0.5\,\mathrm{fm}$), our results correspond to $\Delta E^{\mathrm{HQET}}_{2,1} = 606(35)\,\mathrm{MeV}$ and $617(31)\,\mathrm{MeV}$, respectively.

For the $\mathrm{B_s} - \mathrm{B_s^*}$ mass difference, we find

$$r_0\Delta E_{\mathrm{P-V}} = -0.075(8) \tag{3.11}$$

giving $\Delta E_{\mathrm{P-V}} = -29.8(3.2)\,\mathrm{MeV}$ via $r_0 = 0.5\,\mathrm{fm}$. This is to be contrasted to the experimental value [40] of $m_{\mathrm{B_s}} - m_{\mathrm{B_s^*}} = -49.0(1.5)\,\mathrm{MeV}$. We note that while $\mathrm{O}(1/m_{\mathrm{b}}^2)$ effects

JHEP05(2010)074

may not be entirely negligible for such a small splitting, the difference is too large to be entirely attributed to these. Instead, a genuine quenching effect is involved.

The spin splitting between the first radial excitations in the pseudoscalar and vector channels is

$$r_0 \Delta E_{\mathrm{P}'-\mathrm{V}'} = -0.056(27)\,, \tag{3.12}$$

which is compatible with the spin splitting between the ground states.

Our results confirm the expectation that the $\mathrm{O}(1/m_\mathrm{b})$ contributions are small compared to the static results. To get an idea of the size of higher order corrections in $1/m_\mathrm{b}$, we have considered the dependence of the energy level splittings on the matching conditions chosen in the determination [23] of the HQET parameters ω_kin and ω_spin. We find that the dependence is very minor, with a maximum deviation of $\delta|r_0 \Delta E_{\mathrm{P}-\mathrm{V}}| = 0.005$, less than the statistical errors, and $\delta|r_0 \Delta E_{2,1}^{1/m}| = 0.002$, much less than the statistical errors. Comparing this to the naive power counting estimate of $|O(1/m_\mathrm{b}^2)| \sim 1/(r_0 m_\mathrm{b})^2 \sim 1/100$, we see that the tested $1/m_\mathrm{b}^2$ terms are as small as expected or even smaller. Note that $1/r_0 \approx 400\,\mathrm{MeV}$ is indeed a typical non-perturbative QCD scale.

4 Conclusions

In this paper, we have reported results from quenched lattice QCD for the spectroscopy of the low-lying excited states of the $\mathrm{B_s}$ and $\mathrm{B_s^*}$ systems. An application of the generalized eigenvalue method with all-to-all propagators to non-perturbative HQET at $\mathrm{O}(1/m_\mathrm{b})$ allows us to extract precise results for the energies of the lowest-lying radial excitations as well as for the $\mathrm{B_s} - \mathrm{B_s^*}$ splitting. However, we emphasize again that a careful analysis of systematic errors due to excited state contaminations is necessary.

A first relevant observation to be pointed out concerns the renormalizability of HQET. Unlike for QCD on and off the lattice, there is no proof of renormalizability of the theory to all orders of perturbation theory. However, we find that in our non-perturbative computations the divergences cancel after proper renormalization of HQET [23]. The left over lattice-spacing dependence in figure 2, figure 3 is very flat. To appreciate this, note that

$$r_0^2 E_1^\mathrm{kin} \approx (24\,,\ 47\,,\ 77) \text{ for } a = (0.1\,,\ 0.08\,,\ 0.05) \text{ fm} \tag{4.1}$$

as seen in table 3 and weaker but still very prominent divergences are present in E_n^stat. In other words we find strong numerical evidence for the renormalizability of the theory; in fact also the universality of the continuum limit is demonstrated in the figures. It is also worth emphasizing that the present demonstration is the first time the continuum limit is taken for mass splittings in HQET.

We find the physical $\mathrm{O}(1/m_\mathrm{b})$ corrections to be small throughout.

The precision attained, in particular when taken together with the relative smallness of the $\mathrm{O}(1/m_\mathrm{b})$ effects, indicates that non-perturbative HQET combined with the use of the GEVP for data analysis is a reliable method for determining B meson spectra. We intend to apply it to the $N_\mathrm{f} = 2$ case in the near future. In this context one should remark that we were able to achieve good precision using only 100 configurations in our quenched

JHEP05(2010)074

study. Therefore we do expect to be able to decrease the errors for dynamical fermions. However the influence of topological modes being updated only slowly [41] needs to be controlled or better algorithms with a faster decorrelation need to be used. A promising proposal has been made in [42].

Acknowledgments

We thank Jochen Heitger and Patrick Fritzsch for useful communications.

This work is supported by the Deutsche Forschungsgemeinschaft in the SFB/TR 09, and by the European community through EU Contract No. MRTN-CT-2006-035482, "FLAVIAnet". N.G. acknowledges financial support from the MICINN grant FPA2006-05807, the Comunidad Autónoma de Madrid programme HEPHACOS P-ESP-00346, and participates in the Consolider-Ingenio 2010 CPAN (CSD2007-00042). T.M. thanks the A. von Humboldt Foundation for support.

A All-to-all propagators

In this appendix, we explain the details of our implementation of all-to-all propagators, which follows the idea of [34] with some useful improvements.

A.1 Even-odd preconditioning

To reduce the computational effort and storage requirement for the matrix inversions, we consider even-odd preconditioning of the (hermitian) Wilson-Dirac operator $Q = 2\kappa\gamma_5 D$. With even/odd ordering of the sites one has a block structure

$$Q = \gamma_5 \begin{pmatrix} M_{ee} & M_{eo} \\ M_{oe} & M_{oo} \end{pmatrix} ,$$

where M_{ee} (M_{oo}) differs from unity by the clover term on the even (odd) sites, and M_{oe} (M_{eo}) is the hopping term. Defining

$$B \equiv \begin{pmatrix} \mathbb{1}_e & -M_{ee}^{-1} M_{eo} \\ 0 & \mathbb{1}_o \end{pmatrix} ,$$

the preconditioned matrix $B^\dagger Q B$ is block-diagonal and the propagator can be factorized as

$$Q^{-1} = B \begin{pmatrix} \hat{Q}_{ee}^{-1} & 0 \\ 0 & \hat{Q}_{oo}^{-1} \end{pmatrix} B^\dagger , \tag{A.1}$$

where $\hat{Q}_{ee} = \gamma_5 M_{ee}$ is diagonal in space-time, and $\hat{Q}_{oo} = \gamma_5 (M_{oo} - M_{oe} M_{ee}^{-1} M_{eo}) = \hat{Q}_{oo}^\dagger$.

JHEP05(2010)074

A.2 Approximate low modes and a stochastic estimator

We consider an orthonormal basis $\{\hat{v}_i : i = 1 \ldots N_{\mathrm{L}}\}$ of an N_{L} dimensional subspace ($N_{\mathrm{L}} \geq 0$) of all fermion fields which live only on odd sites. Defining the projectors

$$\mathbf{P}_{\mathrm{L}} \equiv \sum_{i=1}^{N_{\mathrm{L}}} \hat{v}_i \cdot \hat{v}_i^{\dagger} \quad \text{and} \quad \mathbf{P}_{\mathrm{H}} \equiv \mathbb{1}_o - \mathbf{P}_{\mathrm{L}}\,,$$

we can write

$$\hat{Q}_{oo}^{-1} = \hat{Q}_{oo}^{-1}(\mathbf{P}_{\mathrm{L}} + \mathbf{P}_{\mathrm{H}}) = \sum_{i=1}^{N_{\mathrm{L}}} (\hat{Q}_{oo}^{-1}\hat{v}_i) \cdot \hat{v}_i^{\dagger} + \hat{Q}_{oo}^{-1}\mathbf{P}_{\mathrm{H}}\,. \tag{A.2}$$

A natural choice for $\hat{v}_i$ are approximate eigenvectors of the low-lying eigenvalues of $\hat{Q}_{oo}$

$$\hat{Q}_{oo}\hat{v}_i = \lambda_i \hat{v}_i + \hat{r}_i\,. \tag{A.3}$$

with $\|\hat{v}_i\| = 1$ and $\hat{v}_i^{\dagger}\hat{r}_k = 0$. Then, the part $\hat{Q}_{oo}^{-1}\mathbf{P}_{\mathrm{L}}$ in (A.2) is expected to approximate the long-distance behaviour of the propagator [34, 43], and the inversions[1] needed in $(\hat{Q}_{oo}^{-1}\hat{v}_i)$ are cheap.

On the other hand, we can introduce a stochastic estimator for $\mathbf{P}_{\mathrm{H}}$. We take random vectors η_i with

$$\langle \eta_{i,\alpha} \rangle_{\eta} = 0\,, \tag{A.4}$$

$$\langle \eta_{i,\alpha}\, \eta^{*}_{j,\beta} \rangle_{\eta} = \delta_{ij}\delta_{\alpha\beta}\,, \tag{A.5}$$

$$\langle \eta_{i,\alpha}\, \eta_{j,\beta} \rangle_{\eta} = 0\,, \tag{A.6}$$

where α, β denote combined (color, Dirac, and site) indices, and $\langle . \rangle_{\eta}$ is the average over η. The relations (A.4)–(A.6) hold, for instance, in the case of a U(1) noise

$$\eta_{i,\alpha} = \exp(i\phi_{i,\alpha})\,,$$

where $\phi_{i,\alpha}$ are independently uniformly distributed in $[0, 2\pi)$ (while for Z_2 noise the average in (A.6) would not vanish for $i = j$). Thus, the second term in (A.2) can be written as

$$\hat{Q}_{oo}^{-1}\,\mathbf{P}_{\mathrm{H}} = \frac{1}{N_{\eta}} \sum_{i=1}^{N_{\eta}} \left\langle \hat{Q}_{oo}^{-1}\,\mathbf{P}_{\mathrm{H}}\,\eta_i \cdot \eta_i^{\dagger} \right\rangle_{\eta}\,, \tag{A.7}$$

and the estimator of $\hat{Q}_{oo}^{-1}$ can be written as a sum of dyadic products

$$\hat{Q}_{oo}^{-1} = \sum_{i=1}^{N_{\mathrm{L}}+N_{\eta}} \left\langle \hat{w}_i \cdot \hat{u}_i^{\dagger} \right\rangle_{\eta}\,, \tag{A.8}$$

with[2]

$$\begin{aligned} \hat{w}_i &= \hat{Q}_{oo}^{-1}\,\hat{u}_i\,, \qquad \hat{u}_i = \hat{v}_i \qquad (i = 1, \ldots, N_{\mathrm{L}}) \\ \hat{w}_i &= \hat{Q}_{oo}^{-1}\,\mathbf{P}_{\mathrm{H}}\,\hat{u}_i\,, \quad \hat{u}_i = {N_{\eta}}^{-1/2}\,\eta_i \quad (i = N_{\mathrm{L}}{+}1, \ldots, N_{\mathrm{L}}{+}N_{\eta}) \end{aligned}$$

[1] Since we do not explicitly use $\hat{Q}_{oo}^{-1}\hat{v}_i \approx \lambda_i^{-1}\hat{v}_i$, the errors $\|\hat{r}_i\|$ in (A.3) are allowed to be large. In practice, we require $\|\hat{r}_i\| \leq 0.001 \cdot |\lambda_i|$, and take $\lambda_i^{-1}\hat{v}_i$ only as start vectors for the inversion.

[2] One may also use $\hat{w}_i = \hat{Q}_{oo}^{-1}\,\hat{u}_i$ and $\hat{u}_i = {N_{\eta}}^{-1/2}\,\mathbf{P}_{\mathrm{H}}\,\eta_i$ for $i = N_{\mathrm{L}}{+}1, \ldots, N_{\mathrm{L}}{+}N_{\eta}$, but we have not tested this option.

JHEP05(2010)074

The full propagator Q^{-1} is then obtained from (A.1). Since B connects only adjacent time slices, the block $\hat{Q}_{ee}^{-1}$ does not contribute to the propagator between sites with time separation $|x_0 - y_0| > 2a$. In this case, we can simply write

$$Q^{-1} = \sum_{i=1}^{N_{\mathrm{L}}+N_\eta} \left\langle w_i \cdot u_i^\dagger \right\rangle_\eta , \tag{A.9}$$

with

$$w_i \equiv B \begin{pmatrix} 0 \\ \hat{w}_i \end{pmatrix} \quad \text{and} \quad u_i \equiv B \begin{pmatrix} 0 \\ \hat{u}_i \end{pmatrix} .$$

Even-odd preconditioning can be seen as a form of dilution since there are only half as many components of the noise field η in the even-odd preconditioned case as without preconditioning. Note, however, that unlike other dilution schemes, even-odd preconditioning does not increase the number of inversions needed.

A.3 Time dilution

In addition, we use the more conventional time dilution scheme. It is implemented by replacing $\mathbf{P}_{\mathrm{H}}$ in (A.2) by $\mathbf{P}_{\mathrm{H}} \sum_t \mathbf{P}_t$ where $\mathbf{P}_t$ projects on the components corresponding to (odd) sites with time coordinate t. Then, an independent stochastic estimator is introduced for each term

$$\mathbf{P}_{\mathrm{H}} \mathbf{P}_t = \frac{1}{N_\eta} \sum_{i=1}^{N_\eta} \left\langle (\mathbf{P}_{\mathrm{H}}\, \eta_{ti}) \cdot \eta_{ti}^\dagger \right\rangle_\eta ,$$

where the noise vectors η_{ti} have non-vanishing components only for (odd) sites on time-slice t.

Note that due to the hopping term in B the full propagator (A.9) from time slice x_0 to y_0 receives contributions from noise vectors η_{ti} on three time slices, $t = x_0, x_0 \pm a$, i.e. three inversions are required for the propagator from one time slice x_0. However, a total of T inversions is sufficient, and hence no extra effort is required, if one computes the propagator for all x_0, as we do in our measurements.

Analysing the variance of a heavy-light two-point correlator as described in [44], one sees that the variance with time dilution decays roughly as $\mathrm{e}^{-(x_0-y_0)m_\pi}$, while the expression without time dilution contains pieces independent of $x_0 - y_0$. This renders time dilution very profitable.

References

[1] D0 collaboration, V.M. Abazov et al., *Observation and properties of the orbitally excited B_{s2}^* meson*, *Phys. Rev. Lett.* **100** (2008) 082002 [arXiv:0711.0319] [SPIRES].

JHEP05(2010)074

[2] D0 collaboration, V.M. Abazov et al., *Observation and properties of $L = 1 B_1$ and B_2^* mesons*, *Phys. Rev. Lett.* **99** (2007) 172001 [arXiv:0705.3229] [SPIRES].

[3] CDF collaboration, T. Aaltonen et al., *Measurement of resonance parameters of orbitally excited narrow B^0 mesons*, *Phys. Rev. Lett.* **102** (2009) 102003 [arXiv:0809.5007] [SPIRES].

[4] CDF collaboration, T. Aaltonen et al., *Observation of orbitally excited B_s mesons*, *Phys. Rev. Lett.* **100** (2008) 082001 [arXiv:0710.4199] [SPIRES].

[5] CDF and D0 collaboration, W. Taylor, *Spectroscopy of B-like hadrons at the Tevatron*, *Nucl. Phys. Proc. Suppl.* **186** (2009) 351 [SPIRES].

[6] M. Wingate, J. Shigemitsu, C.T.H. Davies, G.P. Lepage and H.D. Trottier, *Heavy-light mesons with staggered light quarks*, *Phys. Rev.* **D 67** (2003) 054505 [hep-lat/0211014] [SPIRES].

[7] J. Foley, A. O'Cais, M. Peardon and S.M. Ryan, *Radial and orbital excitations of static-light mesons*, *Phys. Rev.* **D 75** (2007) 094503 [hep-lat/0702010] [SPIRES].

[8] UKQCD collaboration, J. Koponen, *Energies of B_s meson excited states: a Lattice study*, *Phys. Rev.* **D 78** (2008) 074509 [arXiv:0708.2807] [SPIRES].

[9] ETM collaboration, K. Jansen, C. Michael, A. Shindler and M. Wagner, *The Static-light meson spectrum from twisted mass lattice QCD*, *JHEP* **12** (2008) 058 [arXiv:0810.1843] [SPIRES].

[10] T. Burch, C. Hagen, C.B. Lang, M. Limmer and A. Schafer, *Excitations of single-beauty hadrons*, *Phys. Rev.* **D 79** (2009) 014504 [arXiv:0809.1103] [SPIRES].

[11] E. Eichten and B.R. Hill, *An effective field theory for the calculation of matrix elements involving heavy quarks*, *Phys. Lett.* **B 234** (1990) 511 [SPIRES].

[12] N. Isgur and M.B. Wise, *Weak decays of heavy mesons in the static quark approximation*, *Phys. Lett.* **B 232** (1989) 113 [SPIRES].

[13] H. Georgi, *An effective field theory for heavy quarks at low-energies*, *Phys. Lett.* **B 240** (1990) 447 [SPIRES].

[14] E. Eichten and B.R. Hill, *Static effective field theory: $1/m$ corrections*, *Phys. Lett.* **B 243** (1990) 427 [SPIRES].

[15] M. Antonelli et al., *Flavor physics in the quark sector*, arXiv:0907.5386 [SPIRES].

[16] C. Michael and I. Teasdale, *Extracting glueball masses from lattice QCD*, *Nucl. Phys.* **B 215** (1983) 433 [SPIRES].

[17] M. Lüscher and U. Wolff, *How to calculate the elastic scattering matrix in two-dimensional quantum field theories by numerical simulation*, *Nucl. Phys.* **B 339** (1990) 222 [SPIRES].

[18] G.P. Lepage et al., *Constrained curve fitting*, *Nucl. Phys. Proc. Suppl.* **106** (2002) 12 [hep-lat/0110175] [SPIRES].

[19] G.M. von Hippel, R. Lewis and R.G. Petry, *Evolutionary fitting methods for the extraction of mass spectra in lattice field theory*, *Comput. Phys. Commun.* **178** (2008) 713 [arXiv:0707.2788] [SPIRES].

[20] B. Blossier, M. Della Morte, G. von Hippel, T. Mendes and R. Sommer, *On the generalized eigenvalue method for energies and matrix elements in lattice field theory*, *JHEP* **04** (2009) 094 [arXiv:0902.1265] [SPIRES].

JHEP05(2010)074

[21] ALPHA collaboration, J. Heitger and R. Sommer, *Non-perturbative heavy quark effective theory*, *JHEP* **02** (2004) 022 [hep-lat/0310035] [SPIRES].

[22] M. Della Morte, N. Garron, M. Papinutto and R. Sommer, *Heavy quark effective theory computation of the mass of the bottom quark*, *JHEP* **01** (2007) 007 [hep-ph/0609294] [SPIRES].

[23] B. Blossier, M. Della Morte, N. Garron and R. Sommer, *HQET at order* $1/m$*: I. Non-perturbative parameters in the quenched approximation*, arXiv:1001.4783 [SPIRES].

[24] M. Della Morte, P. Fritzsch, J. Heitger and R. Sommer, *Non-perturbative quark mass dependence in the heavy-light sector of two-flavour QCD*, PoS(LATTICE 2008)226 [arXiv:0810.3166] [SPIRES].

[25] R. Sommer, *Non-perturbative renormalization of HQET and QCD*, *Nucl. Phys. Proc. Suppl.* **119** (2003) 185 [hep-lat/0209162] [SPIRES].

[26] M. Della Morte, A. Shindler and R. Sommer, *On lattice actions for static quarks*, *JHEP* **08** (2005) 051 [hep-lat/0506008] [SPIRES].

[27] B.A. Thacker and G.P. Lepage, *Heavy quark bound states in lattice QCD*, *Phys. Rev.* **D 43** (1991) 196 [SPIRES].

[28] A. Hasenfratz and F. Knechtli, *Flavor symmetry and the static potential with hypercubic blocking*, *Phys. Rev.* **D 64** (2001) 034504 [hep-lat/0103029] [SPIRES].

[29] A. Hasenfratz, R. Hoffmann and F. Knechtli, *The static potential with hypercubic blocking*, *Nucl. Phys. Proc. Suppl.* **106** (2002) 418 [hep-lat/0110168] [SPIRES].

[30] B. Sheikholeslami and R. Wohlert, *Improved continuum limit lattice action for QCD with Wilson fermions*, *Nucl. Phys.* **B 259** (1985) 572 [SPIRES].

[31] M. Lüscher, S. Sint, R. Sommer, P. Weisz and U. Wolff, *Non-perturbative* $O(a)$ *improvement of lattice QCD*, *Nucl. Phys.* **B 491** (1997) 323 [hep-lat/9609035] [SPIRES].

[32] ALPHA collaboration, J. Garden, J. Heitger, R. Sommer and H. Wittig, *Precision computation of the strange quark's mass in quenched QCD*, *Nucl. Phys.* **B 571** (2000) 237 [hep-lat/9906013] [SPIRES].

[33] R. Sommer, *A New way to set the energy scale in lattice gauge theories and its applications to the static force and* α_s *in* SU(2) *Yang-Mills theory*, *Nucl. Phys.* **B 411** (1994) 839 [hep-lat/9310022] [SPIRES].

[34] J. Foley et al., *Practical all-to-all propagators for lattice QCD*, *Comput. Phys. Commun.* **172** (2005) 145 [hep-lat/0505023] [SPIRES].

[35] S. Güsken et al., *Nonsinglet axial vector couplings of the baryon octet in lattice QCD*, *Phys. Lett.* **B 227** (1989) 266 [SPIRES].

[36] **APE** collaboration, M. Albanese et al., *Glueball masses and string tension in lattice QCD*, *Phys. Lett.* **B 192** (1987) 163 [SPIRES].

[37] S. Basak et al., *Combining quark and link smearing to improve extended baryon operators*, PoS(LAT2005)076 [hep-lat/0509179] [SPIRES].

[38] F. Niedermayer, P. Rufenacht and U. Wenger, *Fixed point gauge actions with fat links: scaling and glueballs*, *Nucl. Phys.* **B 597** (2001) 413 [hep-lat/0007007] [SPIRES].

[39] B. Blossier et al., *Spectroscopy and decay constants from nonperturbative HQET at order* $1/m$, arXiv:0911.1568 [SPIRES].

JHEP05(2010)074

[40] C. Amsler et al., *Review of particle physics*, *Phys. Lett.* **B 667** (2008) 1 [SPIRES].

[41] S. Schaefer, R. Sommer and F. Virotta, *Investigating the critical slowing down of QCD simulations*, arXiv:0910.1465 [SPIRES].

[42] M. Lüscher, *Trivializing maps, the Wilson flow and the HMC algorithm*, *Commun. Math. Phys.* **293** (2010) 899 [arXiv:0907.5491] [SPIRES].

[43] H. Neff, N. Eicker, T. Lippert, J.W. Negele and K. Schilling, *On the low fermionic eigenmode dominance in QCD on the lattice*, *Phys. Rev.* **D 64** (2001) 114509 [hep-lat/0106016] [SPIRES].

[44] M. Lüscher, *Computational strategies in lattice QCD*, arXiv:1002.4232 [SPIRES].

JHEP05(2010)074